journal of the mechanical behavior of biomedical materials 125 (2022) 104965

Contents lists available at ScienceDirect

Journal of the Mechanical Behavior of Biomedical Materials

journal homepage: www.elsevier.com/locate/jmbbm

Research Paper

Decellularised human bone allograft from different anatomical sites as a basis for functionally stratified repair material for bone defects

Halina T. Norbertczak [a,*], Hazel L. Fermor [a], Jennifer H. Edwards [a], Paul Rooney [b], Eileen Ingham [a], Anthony Herbert [c]

[a] Institute of Medical and Biological Engineering, School of Biomedical Sciences, Faculty of Biological Sciences, University of Leeds, Leeds, United Kingdom
[b] NHS Blood and Transplant Tissue and Eye Services, Liverpool, United Kingdom
[c] Institute of Medical and Biological Engineering, School of Mechanical Engineering, Faculty of Engineering and Physical Sciences, University of Leeds, Leeds, United Kingdom

ARTICLE INFO

Keywords:
Decellularisation
Trabecular bone
Tissue scaffolds
Femoral head
Tibial plateau

ABSTRACT

Tissue engineered bone solutions aim to overcome the limitations of autologous and allogeneic grafts. Decellularised tissues are produced by washing cellular components from human or animal tissue to produce an immunologically safe and biocompatible scaffold, capable of integration following implantation. A decellularisation procedure utilising low concentration sodium dodecyl sulphate (0.1% w/v) was applied to trabecular bone from human femoral heads (FH) and tibial plateaus (TP). Biological (histology, DNA quantification), biomechanical (compression testing) and structural (μCT) comparisons were made between decellularised and unprocessed cellular tissue. Total DNA levels of decellularised FH and TP bone were below 50 ng mg^{-1} dry tissue weight and nuclear material was removed. No differences were found between cellular and decellularised bone, from each anatomical region, for all the biomechanical and structural parameters investigated. Differences were found between cellular FH and TP and between decellularised FH and TP. Decellularised FH had a higher ultimate compressive stress, Young's modulus and 0.2% proof stress than decellularised TP ($p = 0.001$, 0.002, 0.001, Mann Whitney *U* test, MWU). The mineral density of cellular and decellularised TP bone was significantly greater than cellular and decellularised FH bone respectively (cellular: $p = 0.001$, decellularised: $p < 0.001$, MWU). The bone volume fraction and trabecular thickness of cellular and decellularised FH bone were significantly greater than cellular and decellularised TP bone respectively (cellular: $p = 0.001$, 0.005; decellularised: $p < 0.001$, <0.001, MWU). Characterisation of decellularised trabecular bone from different anatomical regions offers the possibility of product stratification, allowing selection of biomechanical properties to match particular anatomical regions undergoing bone graft procedures.

1. Introduction

Bone grafts are utilised in a wide range of surgical procedures including joint replacements surgeries; spinal fusions; dental and craniofacial surgeries; treatment of non-union fractures and replacement of bone stock, lost due to cancers or trauma (Board et al., 2006; Elsalanty and Genecov, 2009; Vaz et al., 2010; Roberts and Rosenbaum, 2012; Kumar et al., 2013; Wee and Thevendran, 2017; Bai et al., 2018). It has been estimated that in the US, between 1992 and 2007, almost 2 million patients received a bone graft as part of their surgical procedure (Kinaci et al., 2014).

The gold standard graft choice is autograft tissue, commonly from the iliac crest (Lomas et al., 2013; Campana et al., 2014). Autograft bone is immunocompatible and has osteoinductive, osteoconductive and osteogenic properties that facilitate bone integration and healing (Khan et al., 2005; Roberts and Rosenbaum, 2012). Donor site morbidity, however, is a possible consequence of this approach along with limitations of the amount of donor bone available and increased surgery times (Roberts and Rosenbaum, 2012; Lomas et al., 2013). Another source of bone is from allografts which, despite tissue screening, still presents a risk of disease transmission and can cause adverse immune responses (Hinsenkamp et al., 2012; Lomas et al., 2013). Demineralised bone

* Corresponding author. Institute of Medical and Biological Engineering, School of Biomedical Sciences, Faculty of Biological Sciences, University of Leeds, Leeds, LS2 9JT, UK.
E-mail address: h.t.norbertczak@leeds.ac.uk (H.T. Norbertczak).

https://doi.org/10.1016/j.jmbbm.2021.104965
Received 3 August 2021; Received in revised form 6 October 2021; Accepted 6 November 2021
Available online 13 November 2021

matrix (DBM), another allograft product, is also a popular choice. Bone morphogenetic proteins within the DBM induce new bone formation (Gruskin et al., 2012; Eagle et al., 2015). However, there can be variation in osteoinductive properties between products from different manufacturers and even between batches from the same manufacturer, due to different production methods and donor tissue variation (Dinopoulos and Giannoudis, 2006; Gruskin et al., 2012; Wee and Thevendran, 2017). Calcium based synthetic bone substitutes are another option (e.g. calcium sulphate, calcium phosphate cements, hydroxyapatite), although biomechanically these are weaker than natural bone and have resorption rates that differ from bone which can negatively impact bone remodelling (Roberts and Rosenbaum, 2012; Sohn and Oh, 2019).

An alternative approach is to utilise xenogeneic or allogeneic bone that is devoid of cells and immunogenic proteins. Allogeneic bone, washed of bone marrow (and associated cells), has been shown to be osteoinductive, exhibit no cytotoxicity and have minimal immunogenicity (Smith et al., 2015, 2017). It is believed that bone integration of allogeneic bone grafts may be accelerated when bone marrow is effectively removed since the presence of dead cells may otherwise inhibit progenitor and osteogenic cells from adhering to the bone and initiating remodelling (Smith et al., 2015). Removal of bone marrow lipid components also prevents these molecules from interfering with revascularisation and incorporation (Thoren et al., 1995; Lomas et al., 2013).

Decellularisation has been successfully applied to a range of xenogeneic or allogeneic tissues for tissue repair and replacement (Gilbert et al., 2006; Crapo et al., 2011). The resulting tissue scaffolds are non immunogenic and retain the collagen rich extracellular matrix, functional molecules and structure (Gilbert et al., 2006). It has been suggested that successful decellularisation is achieved when levels of residual double stranded DNA are less than 50 ng mg^{-1} of dry tissue weight (Crapo et al., 2011). Patented decellularisation methods which utilise low concentration (0.1% w/v) sodium dodecyl sulphate (SDS), protease inhibitors and nucleases to remove cellular components have been shown to reduce the total DNA to below 50 ng mg^{-1} for a range of tissue types and sources (Booth et al., 2002; Wilshaw et al., 2006; Stapleton et al., 2008; Kheir et al., 2011; Hogg et al., 2013; Fermor et al., 2014; Helliwell et al., 2017; Jones et al., 2017; Aldridge et al., 2018; Vafaee et al., 2018; Norbertczak et al., 2020). Decellularised human bone-patella tendon-bone tissue has been implanted into ovine knees as an anterior cruciate ligament replacement for 26 weeks. The grafts showed evidence of constructive remodelling with osseointegration with recipient bone and biomechanical integrity at the host bone interface, illustrating the capacity for the decellularised human bone remodelling to securely anchor the decellularised construct (Edwards et al., 2017).

Femoral head (FH) bone is a common source of bone allograft tissue. NHS Blood and Transplant Tissue and Eye Services (NHS BT TES, Liverpool, UK), for example, supplies a range of FH products for clinical use, issuing c.2500–3000 FHs annually (NHS BT TES bone product catalogue, Lomas et al., 2013; Eagle et al., 2017). It is proposed that decellularised bone, not only from the FH but from other anatomical regions, could be utilised as bone graft materials. Furthermore, bone sourced from different anatomical sites is likely to have different inherent structural and biomechanical properties, facilitating the potential for the stratification of bone graft for various applications. In this study trabecular bone from the FH and tibial plateau (TP) in both its unprocessed "cellular" and processed "decellularised" states was compared.

The primary aim of this investigation was to determine the effects of decellularisation on trabecular bone from two anatomical regions (FH and TP) through comparisons of biomechanical and structural properties of decellularised and cellular bone. The secondary aims were to assess the potential differences in biomechanical and structural properties between cellular FH and TP bone and between decellularised FH and TP bone.

2. Materials and methods

2.1. Tissue procurement

Following ethical approval (London-London Bridge Research Ethics Committee REC ref 18/LO/1534, approval date 3 September 2018) deceased donor tissue taken with informed consent (10 proximal femurs and 11 whole knees from the donor's left leg) was obtained from NHS BT TES, Liverpool, UK. The donor age range was 40–79 years old (mean 60, median 61). There were three female and eight male donors. Tissue was stored at −80 °C post harvest and transferred to −40 °C prior to use in the investigation; it was then thawed overnight to 4 °C and dissected aseptically. Tissue was processed within laboratories under licence from the UK Human Tissue Authority in compliance with the Human Tissue Act of 2004.

2.2. Tissue dissection

Dissection of Femoral Heads: The femoral shaft was held in a vice with the FH uppermost (Fig. 1a). Soft tissue was abraded from the FH and the fovea was cleared for any ligamentous tissue using a scalpel. An oscillating electrical saw (AFM14 FEIN Akku Multimaster) was used to remove the proximal curved surface of the FHs approximately perpendicular to the axis of the femoral neck (Fig. 1b). Pins (8 mm diameter) were drilled from the FH, perpendicular to the exposed trabecular bone surface (two in the anterior aspect and two in the posterior aspect) (Fig. 1c). A slice of approximately 20 mm was then taken though the FH approximately parallel to the initial cut surface to aid bone pin removal (Fig. 1d). In this way four pins were obtained from each quadrant of the FH, 16–20 mm in height (Fig. 1e). Bone pins were stored at −40 °C. Bone pins from either the anterior (four) or posterior aspects (three) of each donor FH were decellularised, while the corresponding posterior (four) and anterior (three) bone pins were retained as donor matched cellular controls.

Dissection of Tibial Plateaus: Whole knees were disarticulated to isolate the TP. The tibial shaft was held in a vice with the TP uppermost (Fig. 1f). Soft tissue was removed from the TP using sterile scalpels and forceps. The saw was used to remove cortical bone and cartilage from the upper surface and sides of the TP (Fig. 1f). Bone pins (8 mm in diameter) were drilled perpendicular to the exposed trabecular bone of TPs, in the medial and lateral aspects of the tissue (Fig. 1g). A slice of approximately 20 mm was then taken though the TP approximately parallel to the cut surface to aid pin removal (Fig. 1h). Up to three pins were obtained from the centre of the medial and lateral side of the TP, 16–20 mm in height (Fig. 1i&j). Bone pins were stored at −40 °C. Bone pins from either the medial (four) or lateral sides (five) of each donor TP were decellularised, while the corresponding lateral (four) and medial (five) bone pins were retained as donor matched cellular controls.

2.3. Decellularisation protocol

Stored bone pin samples were defrosted to room temperature before undergoing two freeze thaw cycles in hypotonic buffer (10 mM tris, Sigma-Aldrich; 10 $KIU.mL^{-1}$ aprotinin Trasylol, ®, Bayer; pH 8) between −40 °C and room temperature. The freeze thaw cycles were followed by ultrasonication of the submerged sample (10 min, 44 kHz) then centrifugation (15 min, 1900×*g*). Samples were washed in hypotonic buffer followed by hypotonic buffer containing 0.1% w/v SDS (Sigma-Aldrich) for two cycles (16 h for the first wash step and 24 h thereafter). Samples were washed in Dulbecco's phosphate buffered saline, DPBS (Oxoid) containing 10 $KIU.mL^{-1}$ aprotinin for three, 10 min cycles (with changes of fresh solution) followed by a 72 h DPBS cycle. Samples were treated with nuclease solution for two cycles (50 mM tris, Sigma-Aldrich; 1 mM magnesium chloride, VWR International; 10 $U.mL^{-1}$ Benzonase, Novagen; pH 7.5; 37 °C, 80 rpm, 3 h). Samples were then washed in DPBS for three, 10 min cycles (with changes of fresh solution) then

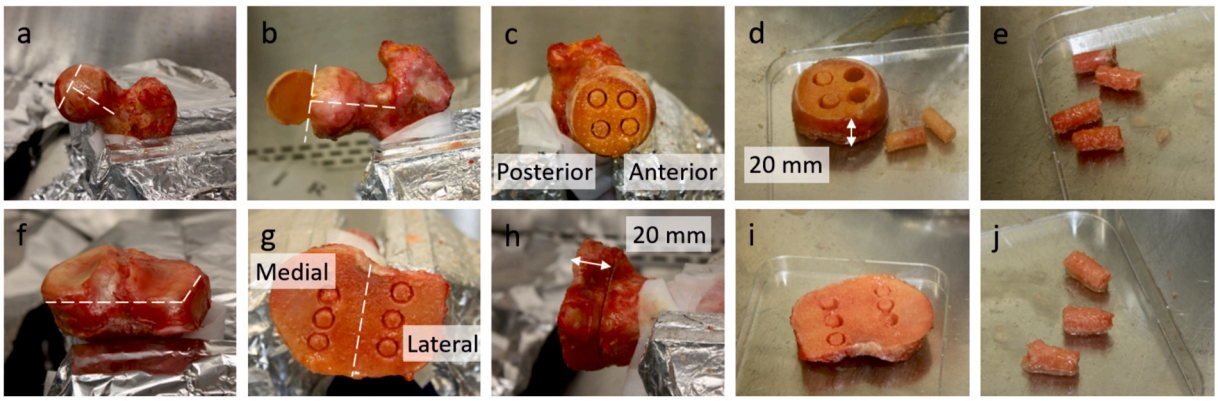

Fig. 1. Stages of tissue dissection. Extraction of trabecular bone pins (8 mm diameter x 16–20 mm height) from the femoral head (a–e) and tibial plateau (f–j).

hypertonic buffer (50 mM tris; 1.5 M sodium chloride, ThermoFisher Scientific; pH 7.5) followed by DPBS for seven cycles (72 h x 2, 168 h, 10 min x 3, 24 h). Unless stated, wash steps were carried out at 42 °C with agitation on an orbital shaker (PSU–10I, Grant bio) at 110 rpm. Sterile solutions were used throughout the protocol and aseptic solution changes were made. Samples were stored at −40 °C until required for further analysis. Samples were decellularised with two bone pins per 100 mL wash solution and 30 mL nuclease solution. Cellular trabecular bone pin samples were retained as control tissue for analyses. Bone pins were stored at −40 °C.

2.4. Quality assurance testing

Decellularised bone pin samples were quality assurance tested to assess the efficacy of the decellularisation protocol.

DNA quantification: Decellularised FH (n = 7) and TP (n = 10) bone pins were compared to cellular FH (n = 6) and TP bone (n = 6) for their total DNA content. Bone pins were freeze-dried to a constant weight and crushed with a pestle and mortar. A DNeasy Blood and Tissue kit (Qiagen), was used according to manufacturer instructions to extract total DNA from known weights of crushed lyophilised samples. The kit tissue digestion buffer was substituted with an in house digestion buffer (12.5% (w/v) ethylenediaminetetraacetic acid, EDTA; 1% (w/v) SDS) and was used with the proteinase K enzyme provided in the kit (600 mAU/ml). Spectrophotometric quantification of the extracted DNA was carried out (Nanodrop ND-1000, Labtech International) and results expressed in $ng.mg^{-1}$ of dry tissue weight.

Histological evaluation: Decellularised FH (n = 7) and TP (n = 10) bone pins were compared to cellular FH (n = 7) and TP bone (n = 10). Samples were fixed for 48 h in 10% (v/v) neutral buffered formalin, NBF (Atom Scientific); demineralised in 12.5% (w/v) EDTA (Fisher Scientific), pH 7 at 42 °C and 120 rpm for ten days. Samples were fixed again (48 h); processed automatically (Leica TP1020 tissue processor, Leica Biosystems); cut in half and embedded in paraffin wax with the cut surface orientated to the outer face of the wax block. Mayer's haematoxylin and Eosin Y, (H&E; Atom Scientific and Merck Millipore respectively) or 4′, 6-diamidino-2-phenylindole (DAPI; Sigma-Aldrich) was used to stain 5 μm thick histological sections.

2.5. Structural evaluation

Cellular and decellularised FH (n = 7 cellular and decellularised) and TP (n = 9, cellular and decellularised) bone pins were defrosted to 4 °C in transport medium (Hanks balanced salt solution, HBSS with Ca^{+}, $Mg^{2+,}$ $NaCHO_3$ and phenol red, Sigma-Aldrich; 0.01 M HEPES, Sigma-Aldrich and 20 KIU/mL Aprotinin). Bone pins, fully immersed in the transport medium, were scanned using a micro computed tomography (μCT) scanner (μCT 100, Scanco Medical AG) with the following scanner settings: voltage 70 kV, current 114 mA and integration time 250 ms. A 16 μm nominal scanning resolution was also employed. After obtaining the image data, a cylindrical region of interest (ROI) 10 mm in height was defined for the central region of each bone pin specimen. For each sample, the mineralised bone phase in the ROI was segmented through grayscale thresholding of image data, based on the image grayscale histogram. The best-fit segmentation was obtained considering the entire image stack rather than a single slice. Using the scanner-manufacturer provided scripts, the following parameters were established from the segmented ROI image data: mineral density (MD) of the bone volume (BV) in mg hydroxyapatite (HA).cm^{-3} (determined relative to a calibration phantom); bone volume fraction (bone volume/total volume, BV/TV); trabecular connectivity (Tb-c, $1.mm^{-3}$); trabecular number (Tb-n, $1.mm^{-1}$); trabecular thickness (Tb-t, mm); and trabecular spacing (Tb-s, mm). The degree of anisotropy, along with associated eigenvalues (H1, H2 and H3), were also determined. Samples were matched such that decellularised tissue from the FH or TP was compared to cellular tissue from the same donor FH or TP. Following scanning, samples were stored overnight in transport medium at 4 °C before biomechanical evaluation.

2.6. Biomechanical property evaluation

Cellular and decellularised bone pins (FH n = 7; TP n = 9) underwent uniaxial compression testing to determine their biomechanical properties. The ends of the bone pins were trimmed with a scalpel until approximately parallel to each other and filed flat using grinding paper. The height of the bone pin was measured using digital Vernier callipers and the ends fixed into Delrin® plastic endcaps with trace amounts of poly-methyl methacrylate (PMMA) cement (WHW Plastics Ltd.). Samples were placed between the compression platens of an Instron materials testing machine (Instron 3365, Instron), equipped with a 500 N load cell and a DPBS bath maintained at 37 °C (Fig. 2). The upper platen was lowered to contact the upper end cap with a load of 0.5 N. The DPBS bath was raised into place and the specimen was left to equilibrate to temperature for 10 min. Bone pins were cyclically loaded between 0 N and 0.006 strain for 30 cycles at a rate of 0.001 s^{-1}, followed by a ramp to failure at the same rate. Data were recorded at a frequency of 10 Hz. The following biomechanical properties for each specimen was determined: ultimate compressive stress (UCS, MPa), Young's modulus (MPa) and 0.2% proof stress (yield stress as determined by a 0.2% offset in the linear region of the stress-strain curve, MPa).

2.7. Data analysis

IBM SPSS Statistics 26 was used to perform statistical analysis. The Shapiro Wilk test for normality was used to assess for parametric data. As some sample groups were found to contain nonparametric data, the

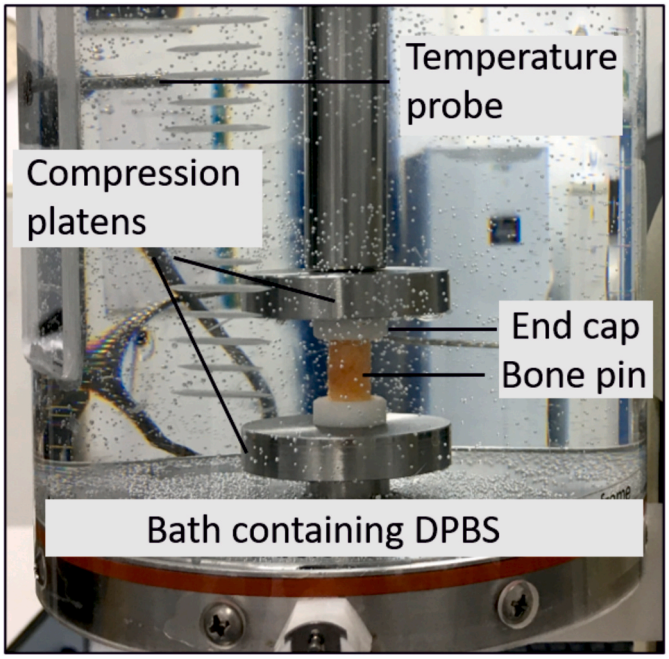

Fig. 2. Compression rig set up. A trabecular bone pin is shown between Delrin® plastic endcaps and compression platens. The sample is shown submerged in 37 °C Dulbecco's phosphate buffered saline (DPBS).

Kruskal Wallace test was used to compare multiple data groups. Where the Kruskal Wallace test produced a significant result ($p < 0.05$), comparisons were made between two sets of unpaired data groups using the Mann Whitney U test as a post hoc test to identify any significant differences between groups. Post hoc testing was limited to comparisons pertinent to the study i.e. cellular v decellularised tissue from each anatomical region (FH and TP); cellular FH v cellular TP and decellularised FH v decellularised TP. The significance level was 0.05. Data in the following bar charts show the mean values with error bars representing 95% confidence intervals.

3. Results

3.1. Quality assurance testing

The mean total DNA levels in both the FH and TP were below 50 ng mg^{-1} dry weight (46.8 ± 9.7 and 35.6 ± 10.4 ng mg^{-1} ± 95% confidence intervals respectively) (Fig. 3). Cell nuclei and bone marrow were largely removed from the central regions of decellularised FH and TP bone pins when compared to cellular tissue; this is shown in the representative images of H&E and DAPI stained histological tissue sections (Figs. 4a & 5 respectively). Additional qualitative observations of the H&E stained histological tissue sections showed that, in the majority of decellularised FH bone pins (4/7) and all cellular FH bone pins, compacted bone and marrow debris was observed below the cut circumference. In contrast most TP bone pins (9/10 decellularised and 7/10 cellular) did not contain such debris. In the rare cases where debris was seen in the TP bone pins, it was present in much smaller amounts than in the FH samples (representative images in Fig. 4b). Images of histological sections also showed that the TP bone had thinner trabeculae and a more open trabecular structure compared to the FH bone (Fig. 4b).

3.2. Biomechanical property evaluation

The UCS, Young's modulus and 0.2% proof stress for cellular and decellularised FH and TP bone pins is shown in Fig. 6. There was significant variation between the four groups investigated (cellular FH, cellular TP, decellularised FH and decellularised TP) for these parameters (UCS $p = 0.003$; Young's modulus $p = 0.022$ and 0.2% proof stress, $p = 0.007$, determined by Kruskal Wallace tests). There were no significant differences in any of the parameters between cellular and decellularised tissue from both anatomical regions (FH and TP), determined by Mann Whitney *U* post hoc tests. The decellularised FH however gave significantly higher values than decellularised TP for UCS ($p = 0.001$); Young's modulus ($p = 0.002$) and 0.2% proof stress ($p = 0.001$) (Mann Whitney U).

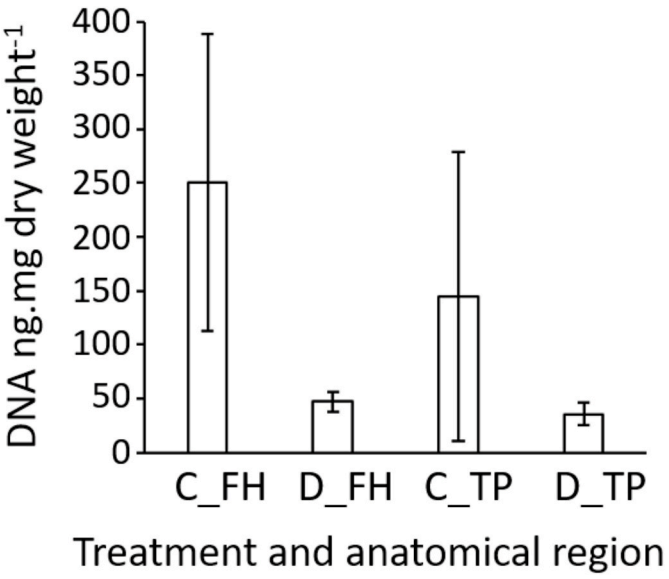

Fig. 3. Mean total DNA content (ng.mg^{-1} dry weight ± 95% confidence intervals) of tissue samples. Cellular femoral head (C_FH), cellular tibial plateau (C_TP), decellularised FH (D_FH) and decellularised TP (D_TP).

3.3. Structural evaluation

The results for the structural analysis parameters (MD, BV/TV, Tb-c, Tb-n, Tb-t and Tb-s) for cellular and decellularised FH and TP are presented in Fig. 7. There was no significant variation between the four groups for Tb-c ($p = 0.101$), Tb-n ($p = 0.072$) and Tb-s ($p = 0.060$) when analysed by Kruskal Wallace tests. There was significant variation between the four groups for MD, BV/TV and Tb-t; $p < 0.001$ for all cases, determined using Kruskal Wallace tests. There were no significant differences between any of the parameters between cellular and decellularised tissue from each anatomical region (FH and TP) when analysed by Mann Whitney *U* post hoc tests. The MD of cellular TP was significantly greater than that of cellular FH ($p = 0.001$) and similarly the MD of decellularised TP was significantly greater that decellularised FH ($p < 0.001$) (Mann Whitney U). BV/TV of cellular FH was significantly greater than that of cellular TP ($p = 0.001$) and BV/TV of decellularised FH was significantly greater that decellularised TP ($p < 0.001$) (Mann Whitney U). The Tb-t of cellular FH was significantly greater than that of cellular TP ($p = 0.005$) and the Tb-t of decellularised FH was significantly greater that decellularised TP ($p < 0.001$) (Mann Whitney U).

The degree of anisotropy for the four groups is shown in Fig. 8a. There was no significant variation between the four groups ($p = 0.404$) as determined using the Kruskal Wallace test; there was no significant difference in the degree of anisotropy indicating that the bone material was orientated to the same extent in all groups. To elucidate the principal direction of bone trabeculae within the sample, eigenvalues produced by the Scanco Medical Systems software were consulted. The principal orientation of bone trabeculae was given by the H2 eigenvalue. The coordinates of the H2 eigenvalue of the TP bone pins predominantly aligned with the z axis of the cartesian coordinate system (i.e. parallel to

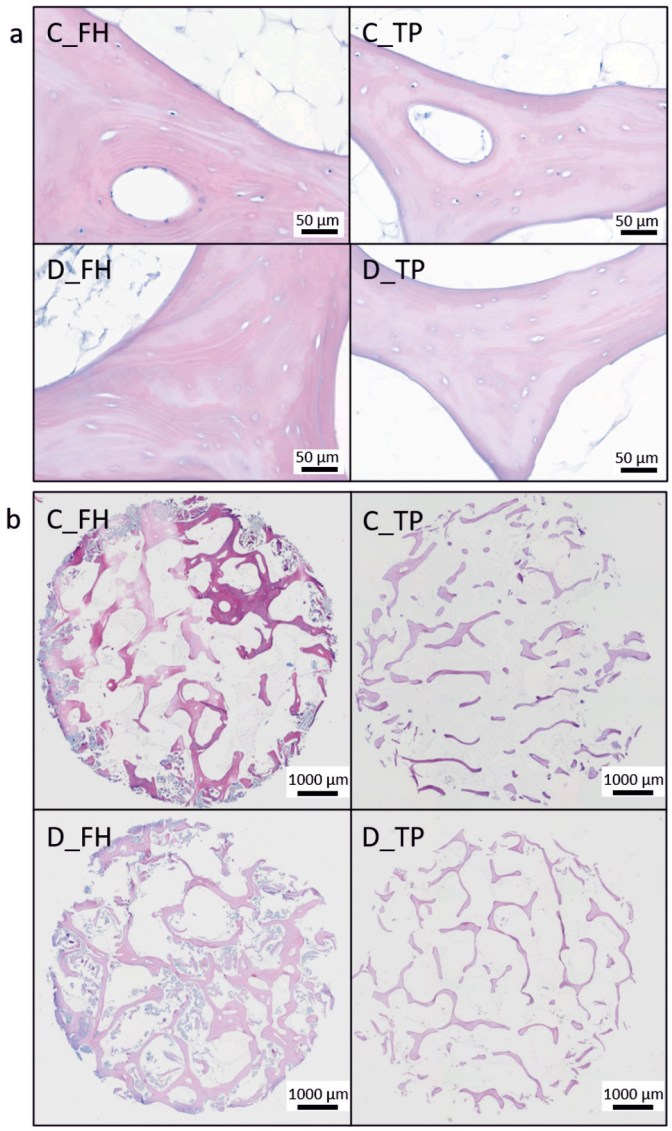

Fig. 4. Images of Haematoxylin and Eosin stained histological tissue sections of trabecular bone pins. Cellular femoral head (C_FH), cellular tibial plateau (C_TP), decellularised FH (D_FH) and decellularised TP (D_TP). Images in 4a were taken at x200 magnification with a 50 μm scale bar and show a lack of purple stained cell nuclei within decellularised trabecular bone. Images in 4b are overview images of the cross section of bone pins and were taken at x25 magnification with a 1000 μm scale bar. (For interpretation of the references to colour in this figure legend, the reader is referred to the Web version of this article.)

the long axis of the bone pin, top to bottom) while the coordinates of the H2 eigenvalue of the FH was aligned 45° diagonally across the long axis of the bone pin. This is depicted in Fig. 8b.

4. Discussion

This study set out to determine the effects of decellularisation on the biomechanical and structural properties of human trabecular bone from the FH and TP. The investigation also assessed the potential differences in these properties between cellular tissue from each anatomical region, and between decellularised tissue from each anatomical region.

Quality assurance testing of the decellularised bone utilised in the investigation showed that trabecular bone from both the FH and TP was successfully decellularised below the recommended target of 50 ng of double stranded DNA per mg of dry tissue weight (Crapo et al., 2011). Almost all the TP bone pins were free of compacted bone debris at their cut circumference. Comparatively more compacted bone debris was observed and in a greater number of both native and decellularised FH samples compared with the TP samples. This difference was likely influenced by the more compact and closed structure of the FH bone preventing the debris from dislodging from within the trabeculae. This bone debris may have acted as a barrier to the infiltration of decellularisation solutions contributing to the higher DNA values observed in the decellularised FH bone.

In the current investigation the geometry of harvested bone (in the form of cylindrical pins) was specifically selected for the biomechanical testing method used. Bone pin harvest involved drilling the bone with a bespoke corer adapted for use with an electrical drill. The continuous motion of the corer against the cut bone surface may have contributed to the compaction of bone debris within trabeculae. Some decellularisation methods utilise DPBS irrigation using a dental flosser (Fermor et al., 2015; Norbertczak et al., 2020); the addition of such a step may help with the removal of debris if not too heavily compacted, for example in the more open structure of the TP. The production of other bone geometries such as cubes, where a closed cutting tool is not used, may result in less compaction of debris at the cut surface. Thus creating little to no barrier to solution infiltration.

No significant differences in the biomechanical properties investigated (UCS, Young's modulus and 0.2% proof stress) were found between cellular tissue and decellularised tissue from the FH or the TP, indicating that decellularisation treatment does not have an effect on bone from these regions. Although there were no significant differences in the UCS, Young's modulus and 0.2% proof stress between cellular FH and TP bone, the values were significantly greater for FH bone compared to TP bone following decellularisation.

Results obtained for the Young's modulus of both FH and TP groups were a factor of 10 lower than results published by Morgan and Keaveny (2001) in which 8 mm cylindrical bone cores from the proximal tibia and femoral neck were harvested in a similar, though not identical, manner and tested at comparable strain rates. The precise area from which the cores were extracted differed between studies. Morgan and Keaveny (2001) specifically extracted samples with the principal trabecular orientation parallel to the long axis of the bone core; in doing so only one core was obtained from each femoral neck, medial proximal tibia and lateral proximal tibia. The current study harvested multiple bone pins from each anatomical region which allowed the production of donor matched in tissue cellular controls and ethical utilisation of donated tissue. This resulted in four off centre bone pins being harvested from each FH quadrant and up to three bone pins taken from each medial and lateral TP. The principal orientation of trabeculae in the FH form plates orthogonal to the articular surface in line with the forces acting through it (Standring, 2021); the harvest strategy of the current investigation resulted in off axis trabecular orientation within the FH bone pins. This was shown by the anisotropy and eigenvalue results which revealed that the principal direction of trabecular orientation was approximately 45 ° to the long axis of the bone pin. In contrast, all TP bone pins in the current study were harvested with the principal alignment of trabeculae parallel to the long axis of the bone pin, though some were harvested from the anterior and posterior aspect of the knee and not from the centre as in the Morgan and Keaveny (2001) study. Other aspects such as age and sex of donors could also have contributed to the differences seen in the results of the two studies. While off axis trabecular orientation for some groups was not ideal, the same method was applied to all groups allowing comparisons to be made, particularly as the goal of the study was to determine the effects of decellularisation on the bone. This was therefore a valid approach.

The geometry of the tested sample and testing conditions are also likely to also influence biomechanical results. For example the Young's modulus and ultimate compressive stress of trabecular bone from bovine humerus were 36 and 18% higher respectively when bone was tested in the form of 5 mm cubes than when in the form of 5 mm diameter x 10

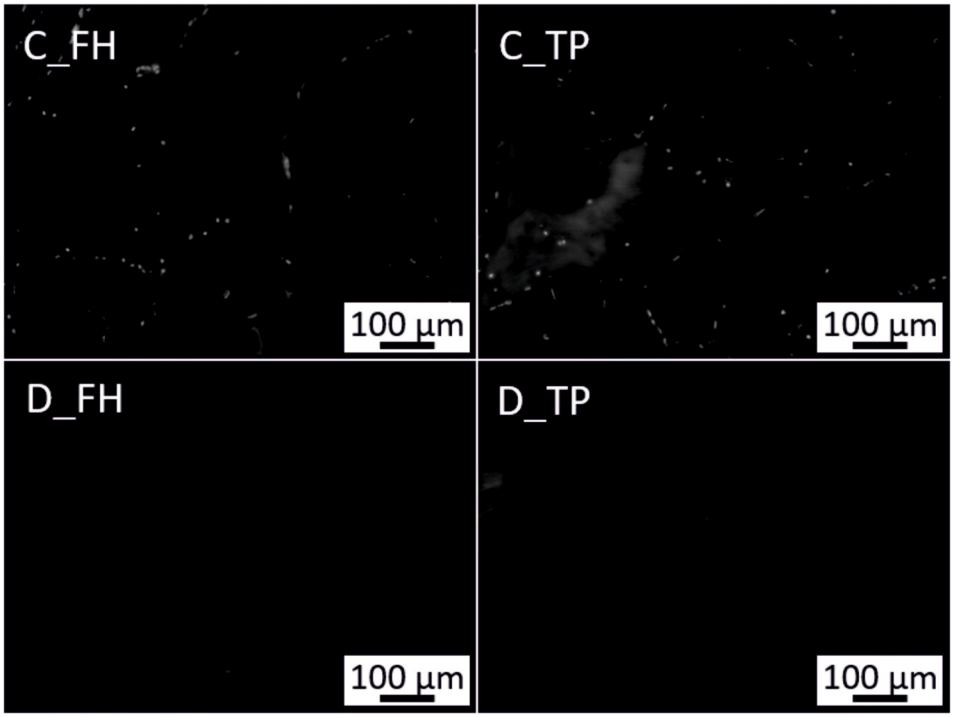

Fig. 5. Images of DAPI stained histological tissue sections of trabecular bone pins. Cellular femoral head (C_FH), cellular tibial plateau (C_TP), decellularised FH (D_FH) and decellularised TP (D_TP). All Images in were taken at x100 magnification with a 100 µm scale bar and illustrate the lack of fluorescing cell nuclei within decellularised trabecular bone.

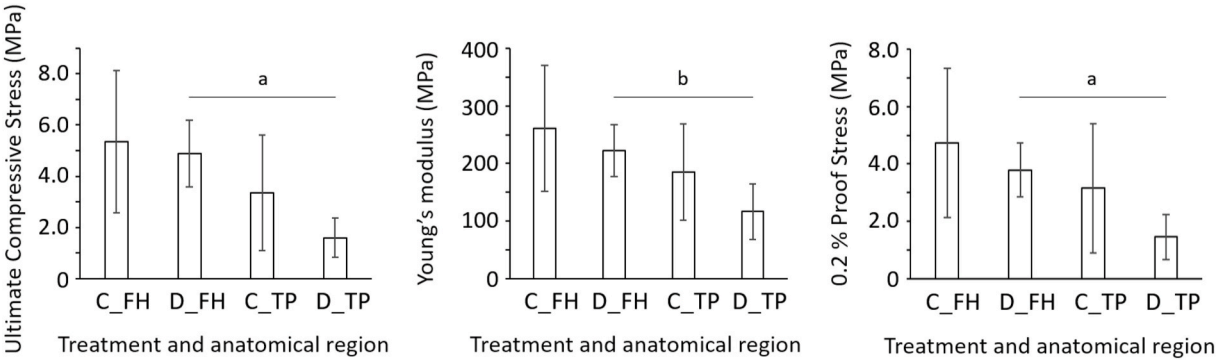

Fig. 6. Comparison of biomechanical property parameters (ultimate compressive stress (UCS, MPa); Young's modulus (MPa) and 0.2% proof stress (MPa)) across test groups (cellular femoral head (C_FH), cellular tibial plateau (C_TP), decellularised FH (D_FH) and decellularised TP (D_TP)). Mean values are shown (±95% confidence intervals). There was significant variation between the four groups for UCS ($p = 0.003$), Youngs modulus, ($p = 0.022$) and 0.2% proof stress ($p = 0.007$) when analysed by Kruskal Wallace tests. Significant differences between groups are shown by labelled bars (a: $p = 0.001$; b: $p = 0.002$, Mann Whitney U).

mm high cylinders (Keaveny et al., 1993). In the study carried out by Eagle et al. (2017) the Young's modulus of 10 mm cubes of unprocessed trabecular bone from the FH was found to be in the region of 60 MPa (10 fold lower than in the current study); this particular study utilised bone cubes as this was the geometry employed for optimisation and development of a bone wash procedure. Furthermore, the bone samples for testing in this investigation were likely to have been randomly selected for biomechanical testing without controlling for, or considering any, trabecular alignment. In optimising bone sample size, geometry and/or location used for specific applications it is not unusual for the resulting properties to differ between studies.

In the current study, differences in biomechanical properties were found between FH and TP bone, with FH bone having greater values for all investigated parameters. The literature supports this observation; Morgan and Keaveny (2001) found higher values for Young's modulus and yield stress in the proximal femur than the proximal tibia. Even within the proximal femur differences were found, with the greater trochanter showing much lower values for each parameter than the femoral neck.

The use of endcaps in the current study provided closed boundary conditions, ensuring that samples deformed in the central region of the bone pin rather than at the ends where trabeculae are cut and open. Compression testing of trabecular bone fixed between endcaps has been shown to give more reproducible and accurate values for Young's modulus estimations. Compression testing of trabecular bone between platens for example, tends to underestimate the Young's modulus somewhere in the region of 20–40% (Keaveny et al., 1997). This underestimation was shown not to be due to differences in anatomical regions, apparent density or aspect ratio of test samples. The current investigation utilised a similar experimental set up, which utilised endcaps for all samples, thus standardising the method for all groups making more accurate comparisons possible.

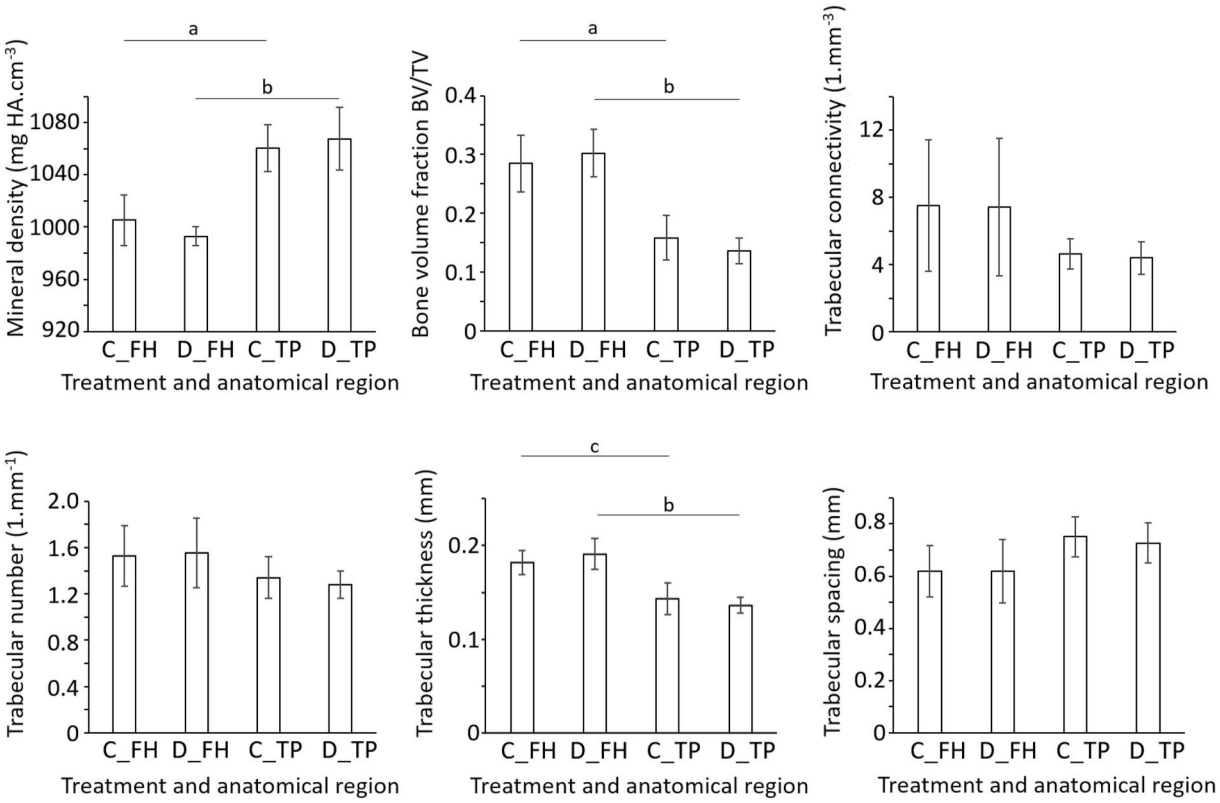

Fig. 7. Comparison of structural data parameters (mineral density (MD, mg HA.cm^{-3}); bone volume fraction (bone volume/total volume, BV/TV); trabecular connectivity (Tb-c, 1.mm^{-3}); trabecular number (Tb-n, 1.mm^{1}); trabecular thickness (Tb-t, mm) and trabecular spacing (Tb-s, mm)) across four test groups (cellular femoral head (C_FH), cellular tibial plateau (C_TP), decellularised FH (D_FH) and decellularised TP (D_TP)). Mean values are shown (±95% confidence intervals). There was no significant variation between the four groups for Tb-c ($p = 0.101$), Tb-n ($p = 0.072$) and Tb-s ($p = 0.060$) when analysed by Kruskal Wallace tests. There was significant variation between the four groups for MD ($p < 0.001$), BV/TV ($p < 0.001$) and Tb-t ($p < 0.001$) when analysed by Kruskal Wallace tests. Significant differences between groups are shown by labelled bars (a: $p = 0.001$; b: $p < 0.001$; c: $p = 0.005$, Mann Whitney U).

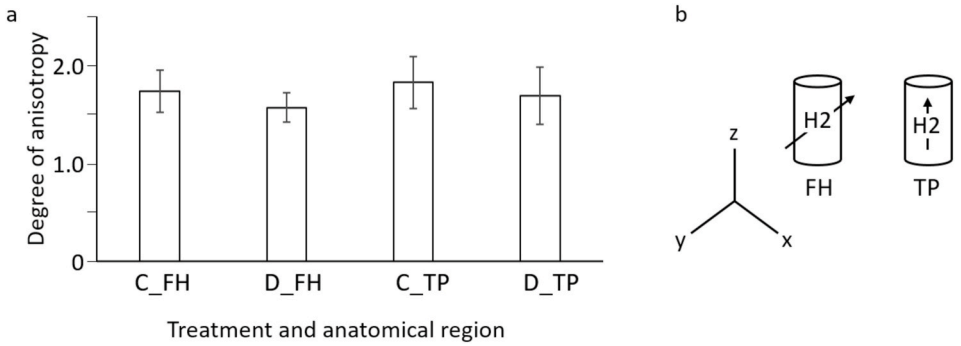

Fig. 8. Mean degree of anisotropy values (±95% confidence intervals) (8a). There was no significant variation between the groups ($p = 0.404$) as determined using the Kruskal Wallis test. Fig. 8b Illustrates the principal direction of bone trabeculae as determined by the H2 eigenvalue.

No significant differences in any of the structural parameters investigated (MD, BV/TV, Tb-c, Tb-n, Tb-t and Tb-s) were found between cellular and decellularised bone of the FH and cellular and decellularised bone of the TP. Decellularisation treatment did not affect the structural properties. MD of the TP was found to be significantly greater than for FH, for both cellular and decellularised bone. The BV/TV and Tb-t of the FH was significantly greater than that of TP for both cellular and decellularised bone. No significant differences were found between any of the groups for Tb-c, Tb-n or Tb-s. Any changes in the structural properties observed between groups, therefore, was likely due to anatomical location rather than the decellularisation process.

It is possible to make some inferences on the relationships between biomechanical and structural parameters based on the available data. Though the MD of FH bone was lower than in the TP, the FH bone had an increased bone volume in a given amount of bone (BV/TV): due to thicker trabeculae (Tb-t) and possibly more trabeculae (Tb-n) and reduced trabecular spacing (Tb-s). These observations may explain why the UCS, Young's modulus and 0.2% proof stress were higher in the FH with BV/TV being a better predictor of/or contributor to the biomechanical properties than MD. Indeed it is also possible that these structural differences also accounted for the increased difficulty in decellularising FH bone compared to TP bone.

Future work will investigate if the differences seen in biomechanical and structural properties of decellularised FH and TP bone are functionally relevant to clinical application. During allografting of bone used in joint replacement surgery bone is morselised and compacted into the

donor site (Board et al., 2006, 2008). Functional testing of morselised decellularised bone will be carried out under clinically relevant conditions of combined compression and shear (Brewster et al., 1999; Albert et al., 2008; McKenna et al., 2013). It may be that bone from each anatomical region (FH and TP) performs in the same manner when morselised, compacted and tested under these conditions. If so, this may suggest that the anatomical location of the allograft is not important for the bone's performance under clinical conditions. Such findings may facilitate the uptake in use of donor bone from a range of anatomical regions and so encourage the utilisation of bone from a broader range of anatomical sites. This may ease any potential supply and demand limitations. Alternatively, there may be differences in the way in which the bone from different locations compacts (for example due to differences in Tb-t), resulting in differences in the compacted aggregate. This in turn may result in different functional performance, meaning that bone sourced from one anatomical region may be better suited to a particular clinical application. It is conceivable that less compacted, more porous bone aggregate may be able to integrate with recipient bone quicker, facilitating increased infiltration of osteoclasts and osteocytes for subsequent bone remodelling. The geometry of morselised bone particles to be used and level of impaction may also be critical in functional performance, perhaps even to the extent whereby correct choice of geometry and compaction alleviate perceived deficiencies in bone from a less considered anatomical source.

5. Conclusion

Decellularisation treatment does not affect biomechanical and structural properties of trabecular bone. Different biomechanical properties were found for decellularised FH and decellularised TP bone indicating that it may be possible to produce decellularised tissue scaffolds with a range of biomechanical properties (functionally stratified) that can be selected for particular graft applications; for example, bone with lower biomechanical properties may be sufficient for use in void filling in fusion cages where the graft material does not have a direct weight bearing function. It has yet to be established whether these differences have any influence on the functional properties of bone when it is morselised and compacted for surgical procedures such as arthroplasty.

Sources of funding

This work was funded through the Medical Technologies Innovation and Knowledge Centre (phase 2 - Regenerative Devices), funded by the Engineering and Physical Sciences Research Council (EPSRC) under grant number EP/N00941X/1 and supported by the EPSRC programme grant: "Optimising knee therapies through improved population stratification and precision of the intervention" (EP/P001076/1). This article presents independent research partially supported by the National Institute for Health Research (NIHR) Leeds Biomedical Research Centre (BRC). The views expressed are those of the author(s) and not necessarily those of the NIHR or the Department of Health and Social Care.

Author statement

Halina Norbertczak: Methodology, Validation, Formal analysis, Investigation, Data Curation, Writing - Original Draft, Writing - Review & Editing, Project administration. Hazel Fermor: Writing - review & editing, Conceptualization, Methodology, Supervision, Funding acquisition. Jenifer Edwards: Methodology, Supervision. Paul Rooney: Conceptualization, Resources, Writing - Review & Editing. Eileen Ingham: Conceptualization, Writing - Review & Editing, Supervision. Anthony Herbert: Conceptualization, Methodology, Formal analysis, Writing - Review & Editing, Supervision, Funding acquisition.

CRediT authorship contribution statement

Halina T. Norbertczak: Data curation, Formal analysis, Investigation, Methodology, Project administration, Validation, Writing – original draft, Writing – review & editing. **Hazel L. Fermor:** Conceptualization, Funding acquisition, Methodology, Supervision, Writing – review & editing. **Jennifer H. Edwards:** Methodology, Supervision. **Paul Rooney:** Conceptualization, Resources, Writing – review & editing. **Eileen Ingham:** Conceptualization, Supervision, Writing – review & editing. **Anthony Herbert:** Conceptualization, Formal analysis, Funding acquisition, Methodology, Supervision, Writing – review & editing.

Declaration of competing interest

☒The authors declare the following financial interests/personal relationships which may be considered as potential competing interests:

Acknowledgements

Professor R.K. Wilcox and Dr G.A. Day for their involvement in discussions on data interpretation; Dr M. Mengoni for advice on statistical analysis and Dr V.N. Wijayathunga for expertise in microcomputed tomography operation and data interpretation. We acknowledge support form NHS BT TES in the provision of donor tissue used in this study and thank the tissue donors and their families. Further data linked to the larger programme of work can be accessed through The Institute of Medical and Biological Engineering Knee Dataset (https://doi.org/10.5518/826).

Appendix A. Supplementary data

Supplementary data to this article can be found online at https://doi.org/10.1016/j.jmbbm.2021.104965.

References

Albert, C., Masri, B., Duncan, C., Oxland, T., Fernlund, G., 2008. Impaction allografting-the effect of impaction force and alternative compaction methods on the mechanical characteristics of the graft. J. Biomed. Mater. Res. B Appl. Biomater. 87 (2), 395–405. https://doi.org/10.1002/jbm.b.31117.

Aldridge, A., Desai, A., Owston, H., Jennings, L.M., Fisher, J., Rooney, P., Kearney, J.N., Ingham, E., Wilshaw, S.P., 2018. Development and characterisation of a large diameter decellularised vascular allograft. Cell Tissue Bank. 19 (3), 287–300. https://doi.org/10.1007/s10561-017-9673-y.

Bai, B., Hao, B., Li, C., Wang, X., 2018. A study of the therapeutic effect of allogeneic bone graft repair following bone tumor resection. Int. J. Clin. Exp. Med. 11 (9), 9544–9551.

Board, T.N., Rooney, P., Kearney, J.N., Kay, P.R., 2006. Impaction allografting in revision total hip replacement. J Bone Joint Surg Br 88, 852–857. https://doi.org/10.1302/0301-620X.88B7.17425.

Board, T., Rooney, P., Kay, P.R., 2008. Strain imparted during impaction grafting may contribute to bony incorporation. J Bone Joint Surg Br 90 (B), 821–824. https://doi.org/10.1302/0301-620X.90B6.20234.

Booth, C., Fisher, J., Ingham, E., 2002. GB2375771A Decellularisation of Matrices.

Brewster, N.T., Gillespie, W.J., Howie, C.R., Madabhushi, S.P.G., Usmani, A.S., Fairbairn, D.R., 1999. Mechanical considerations in impaction bone grafting. J. Bone Joint Surg. 81 (1), 118–124. https://doi.org/10.1302/0301-620x.81b1.8480.

Campana, V., Milano, G., Pagano, E., Barba, M., Cicione, C., Salonna, G., Lattanzi, W., Logroscino, G., 2014. Bone substitutes in orthopaedic surgery: from basic science to clinical practice. J. Mater. Sci. Mater. Med. 25 (10), 2445–2461. https://doi.org/10.1007/s10856-014-5240-2.

Crapo, P.M., Gilbert, T.W., Badylak, S.F., 2011. An overview of tissue and whole organ decellularisation processes. Biomaterials 32 (12), 3233–3243. https://doi.org/10.1016/j.biomaterials.2011.01.057.

Dinopoulos, H.T.H., Giannoudis, P.V., 2006. Safety and efficacy of use of demineralised bone matrix in orthopaedic and trauma surgery. Expet Opin. Drug Saf. (56), 847–866. https://doi.org/10.1517/14740338.5.6.847.

Eagle, M.J., Rooney, P., Kearney, J.N., 2015. Production of an osteoinductive demineralised bone matrix powder without the use of organic solvents. Cell Tissue Bank. 16 (3), 433–441. https://doi.org/10.1007/s10561-014-9487-0.

Eagle, M.J., Man, J., Rooney, P., McQuillan, T.A., Galea, G., Kearney, J.N., 2017. Assessment of a closed wash system developed for processing living donor femoral heads. Cell Tissue Bank. 18 (4), 547–554. https://doi.org/10.1007/s10561-017-9664-z.

Edwards, J.H., Herbert, A., Fermor, H.L., Kearney, J., Rooney, P., Fisher, J., 2017. Regenerative Capacity and Functional Performance of Acellular Human Bone Patellar Tendon Graft in an Ovine Model of Anterior Cruciate Ligament Repair. Orthopaedic Research Society Annual Conference, San Diego, US.

Elsalanty, M.E., Genecov, D.G., 2009. Bone grafts in craniofacial surgery. Craniomaxillofacial Trauma Reconstr. 2 (3), 125–134. https://doi.org/10.1055/s-0029-1215875.

Fermor, H.L., fisher, J., Hasan, J., Ingham, E., Jones, G., 2014. GB2507850A A Decelluralised Implant Material.

Fermor, H.L., Russell, S.L., Williams, S., Fisher, J., Ingham, E., 2015. Development and characterisation of a decellularised bovine osteochondral biomaterial for cartilage repair. J. Mater. Sci. Mater. Med. 26 (186), 1–13. https://doi.org/10.1007/s10856-015-5517-0.

Gilbert, T.W., Sellaro, T.L., Badylak, S.F., 2006. Decellularisation of tissues and organs. Biomaterials 27 (19), 3675–3683. https://doi.org/10.1016/j.biomaterials.2006.02.014.

Gruskin, E., Doll, B.A., Futrell, F.W., Schmitz, J.P., Hollinger, J.O., 2012. Demineralized bone matrix in bone repair: history and use. Adv. Drug Deliv. Rev. 64 (12), 1063–1077. https://doi.org/10.1016/j.addr.2012.06.008.

Helliwell, J.A., Thomas, D.S., Papathanasiou, V., Homer-Vanniasinkam, S., Desai, A., Jennings, L.M., Rooney, P., Kearney, J., NIngham, E., 2017. Development and characterisation of a low-concentration sodium dodecyl sulphate decellularised porcine dermis. J. Tissue Eng. 8, 1–12. https://doi.org/10.1177/2041731417724011.

Hinsenkamp, M., Muylle, L., Eastlund, T., Fehily, D., Noel, L., Strong, D.M., 2012. Adverse reactions and events related to musculoskeletal allografts: reviewed by the World Health Organisation Project NOTIFY. Int. Orthop. 36 (3), 633–641. https://doi.org/10.1007/s00264-011-1391-7.

Hogg, P., Rooney, P., Ingham, E., Kearney, J.N., 2013. Development of a decellularised dermis. Cell Tissue Bank. 14 (3), 465–474. https://doi.org/10.1007/s10561-012-9333-1.

Jones, G., Herbert, A., Berry, H., Edwards, J.H., Fisher, J., Ingham, E., 2017. Decellularisation and characterization of porcine superflexor tendon: a potential anterior cruciate ligament replacement. Tissue Eng. 23 (3–4), 124–134. https://doi.org/10.1089/ten.tea.2016.0114.

Keaveny, T.M., Borchers, R.E., Gibson, L.J., Hayes, W.C., 1993. Trabecular bone modulus and strength can depend on specimen. J. Biomech. 26, 991–1000. https://doi.org/10.1016/0021-9290(93)90059-n.

Keaveny, T.M., Pinilla, T.P., Crawford, R.P., Kopperdahl, D.L., Lou, A., 1997. Systematic and random errors in compression testing of trabecular bone. J. Orthop. Res. 15, 101–110. https://doi.org/10.1002/jor.1100150115.

Khan, S.N., Cammisa, F.P., Sandhu, H.S., Diwan, A.D., Girardi, F.P., Lane, J.M., 2005. The biology of bone grafting. J. Am. Acad. Orthop. Surg. 13, 77–86.

Kheir, E., Stapleton, T., Shaw, D., Jin, Z., Fisher, J., Ingham, E., 2011. Development and characterization of an acellular porcine cartilage bone matrix for use in tissue engineering. J. Biomed. Mater. Res. 99 (2), 283–294. https://doi.org/10.1002/jbm.a.33171.

Kinaci, A., Neuhaus, V., Ring, D.C., 2014. Trends in bone graft use in the United States. Orthopedics 37, 783–788. https://doi.org/10.3928/01477447-20140825-54.

Kumar, P., Vinitha, B., Fathima, G., 2013. Bone grafts in dentisty. J. Pharm. BioAllied Sci. 5, S125–S127. https://doi.org/10.4103/0975-7406.113312.

Lomas, R., Chandrasekar, A., Board, T.N., 2013. Bone allograft in the UK: perceptions and realities. Hip Int. 23 (5), 427–433. https://doi.org/10.5301/hipint.5000018.

McKenna, P.B., Leahy, J.J., Masterson, E.L., McGloughlin, T.M., 2013. Optimizing the fat and water content of impaction bone allograft. J. Orthop. Res. 31 (2), 243–248. https://doi.org/10.1002/jor.22213.

Morgan, E.F., Keaveny, T.M., 2001. Dependence of yield strain of human trabecular bone on anatomic site. J. Biomech. 34, 569–577. https://doi.org/10.1016/s0021-9290(01)00011-2.

NHS BT TES bone product catalogue, Bone products. https://www.nhsbt.nhs.uk/tissue-and-eye-services/products/bone/. (Accessed 4 March 2021).

Norbertczak, H.T., Ingham, E., Fermor, H.L., Wilcox, R.K., 2020. Decellularised intervertebral discs: a potential replacement for degenerate human discs. Tissue Eng. C Methods 26 (11), 565–576. https://doi.org/10.1089/ten.tec.2020.0104.

Roberts, T.T., Rosenbaum, A.J., 2012. Bone grafts, bone substitutes and orthobiologics: the bridge between basic science and clinical advancements in fracture healing. Organogenesis 8 (4), 114–124. https://doi.org/10.4161/org.23306.

Smith, C.A., Richardson, S.M., Eagle, M.J., Rooney, P., Board, T., Hoyland, J.A., 2015. The use of a novel bone allograft wash process to generate a biocompatible, mechanically stable and osteoinductive biological scaffold for use in bone tissue engineering. J Tissue Eng Regen Med 9 (5), 595–604. https://doi.org/10.1002/term.1934.

Smith, C.A., Board, T.N., Rooney, P., Eagle, M.J., Richardson, S.M., Hoyland, J.A., 2017. Human decellularised bone scaffolds from aged donors show improved osteoinductive capacity compared to young donor bone. PLoS One 12 (5), e0177416. https://doi.org/10.1371/journal.pone.0177416.

Sohn, H.S., Oh, J.K., 2019. Review of bone graft and bone substitutes with an emphasis on fracture surgeries. Biomater. Res. 23 (9), 1–7. https://doi.org/10.1186/s40824-019-0157-y.

Standring, S., 2021. Gray's Anatomy, the Anatomical Basis of Clinical Practice, 42nd ed. Elsevier.

Stapleton, T.W., Ingram, J., Katta, J., Knight, R., Korossis, S., Fisher, J., Ingham, E., 2008. Development and characterization of an acellular porcine medial meniscus for use in tissue engineering. Tissue Eng. 14 (4), 505–518. https://doi.org/10.1089/tea.2007.0233.

Thoren, K., Aspenberg, P., Thorngren, K.G., 1995. Lipid extracted bank bone. Bone conductive and mechanical properties. Clin. Orthop. Relat. Res. 311, 232–246.

Vafaee, T., Thomas, D., Desai, A., Jennings, L.M., Berry, H., Rooney, P., Kearney, J., Fisher, J., Ingham, E., 2018. Decellularisation of human donor aortic and pulmonary valved conduits using low concentration sodium dodecyl sulfate. J Tissue Eng Regen Med 12 (2), e841–e853. https://doi.org/10.1002/term.2391.

Vaz, K., Verma, K., Protopsaltis, T., Schwab, F., Lonner, B., Errico, T., 2010. Bone grafting options for lumbar spine surgery: a review examining clinical efficacy and complications. SAS J 4 (3), 75–86. https://doi.org/10.1016/j.esas.2010.01.004.

Wee, J., Thevendran, G., 2017. The role of orthobiologics in foot and ankle surgery: allogenic bone grafts and bone graft substitutes. EFORT Open Rev 2 (6), 272–280. https://doi.org/10.1302/2058-5241.2.160044.

Wilshaw, S.P., Kearney, J.N., Fisher, J., Ingham, E., 2006. Production of an acellular amniotic membrane matrix for use in tissue engineering. Tissue Eng. 12 (8), 2117–2129. https://doi.org/10.1089/ten.2006.12.2117.